Ligand activation of LXRβ reverses atherosclerosis and cellular cholesterol overload in mice lacking LXRα and apoE

Michelle N. Bradley,[1] Cynthia Hong,[1] Mingyi Chen,[1] Sean B. Joseph,[1] Damien C. Wilpitz,[1] Xuping Wang,[2] Aldons J. Lusis,[2] Allan Collins,[3] Willa A. Hseuh,[3] Jon L. Collins,[4] Rajendra K. Tangirala,[3] and Peter Tontonoz[1]

[1]Howard Hughes Medical Institute and Department of Pathology and Laboratory Medicine, [2]Department of Medicine and Department of Human Genetics, and [3]Division of Endocrinology, Department of Medicine, UCLA David Geffen School of Medicine, Los Angeles, California, USA. [4]Nuclear Receptor Discovery Research, GlaxoSmithKline, Research Triangle Park, North Carolina, USA.

Liver X receptors (LXRs) α and β are transcriptional regulators of cholesterol homeostasis and potential targets for the development of antiatherosclerosis drugs. However, the specific roles of individual LXR isotypes in atherosclerosis and the pharmacological effects of synthetic agonists remain unclear. Previous work has shown that mice lacking LXRα accumulate cholesterol in the liver but not in peripheral tissues. In striking contrast, we demonstrate here that *LXRα*$^{-/-}$*apoE*$^{-/-}$ mice exhibit extreme cholesterol accumulation in peripheral tissues, a dramatic increase in whole-body cholesterol burden, and accelerated atherosclerosis. The phenotype of these mice suggests that the level of LXR pathway activation in macrophages achieved by LXRβ and endogenous ligand is unable to maintain homeostasis in the setting of hypercholesterolemia. Surprisingly, however, a highly efficacious synthetic agonist was able to compensate for the loss of LXRα. Treatment of *LXRα*$^{-/-}$*apoE*$^{-/-}$ mice with synthetic LXR ligand ameliorates the cholesterol overload phenotype and reduces atherosclerosis. These observations indicate that LXRα has an essential role in maintaining peripheral cholesterol homeostasis in the context of hypercholesterolemia and provide in vivo support for drug development strategies targeting LXRβ.

Introduction

Cholesterol is a vital component of cell membranes, bile acids, and steroid hormones and is therefore an essential molecule for animal cells. However, elevated cellular levels of free cholesterol are toxic and elevated plasma cholesterol levels increase the risk of atherosclerosis (1, 2). As a result, dysregulation of cholesterol homeostasis at both the cellular and whole-body level is an important contributor to human disease.

The liver X receptors (LXRα and LXRβ) are members of the nuclear receptor superfamily of transcription factors. LXRβ is expressed ubiquitously, while LXRα is predominantly expressed in tissues and cells that play important roles in lipid homeostasis, such as the liver, intestine, adipose tissue, and macrophages. It is now appreciated that both LXR isoforms function as intracellular sensors of cholesterol excess. The natural ligands for both LXRs include oxidized derivatives of cholesterol (oxysterols), such as 22(R)-hydroxycholesterol, and 27-hydroxycholesterol (3–5). Additionally, synthetic LXR ligands have been described that have greater potency and efficacy compared to physiological ligands (e.g., T0901317 and GW3965) (6, 7). The LXR transcription factors form obligate heterodimers with the retinoid X receptor (RXR) and regulate target gene expression through interaction with LXR response elements (LXREs) in the regulatory regions of these genes.

Previous work has demonstrated that LXRs modulate lipid homeostasis through their participation in intestinal cholesterol absorption, conversion of cholesterol to bile acids, reverse cholesterol transport, and lipogenesis (8, 9). Ligand activation of the LXRs has been reported to decrease intestinal cholesterol absorption efficiency (10, 11), induce cholesterol efflux from lipid-laden peripheral cells such as macrophages (11–13), and negatively regulate inflammatory gene expression (14). Each of these effects would be predicted to have a beneficial effect on the development of cardiovascular disease. Indeed, confirmation that the LXR pathway plays a direct role in atherosclerosis susceptibility has been obtained from several studies using mice genetically deficient in LXR expression. LXRα/β double-knockout animals exhibit increased cholesterol accumulation in arterial wall macrophages on a normal chow diet (15). Knockouts of the individual LXRs alone do not display this phenotype, however, indicating that the 2 isotypes can compensate for one another and maintain peripheral cellular cholesterol homeostasis under these conditions. Additional studies have demonstrated that the elimination of both LXRα and LXRβ in the bone marrow compartment results in accelerated atherosclerosis in both spontaneous (*apoE*$^{-/-}$) and diet-induced (*Ldlr*$^{-/-}$) models of the disease (16). On the other hand, activation of LXRs by synthetic agonists has been shown to provide protection against lesion development and to cause regression of established lesions in these models (17–19).

Previous observations that both LXRα and LXRβ regulate expression of ATP-binding cassette transporter A1 (*Abca1*), *Abcg1*, and other target genes in macrophages have supported the view that the 2 LXRs are functionally redundant with respect to the cholesterol efflux pathway (11–13, 15, 20–22). For example, mice lacking LXRα accumulate cholesterol ester in their livers due to a deficiency in *Cyp7A* expression but do not accumulate appreciable levels of cholesterol in peripheral macrophages (22). Furthermore,

Nonstandard abbreviations used: ABC, ATP-binding cassette transporter; LPL, lipoprotein lipase; LXR, liver X receptor.

Conflict of interest: J.L. Collins is an employee of GlaxoSmithKline.

Citation for this article: *J. Clin. Invest.* **117**:2337–2346 (2007). doi:10.1172/JCI31909.

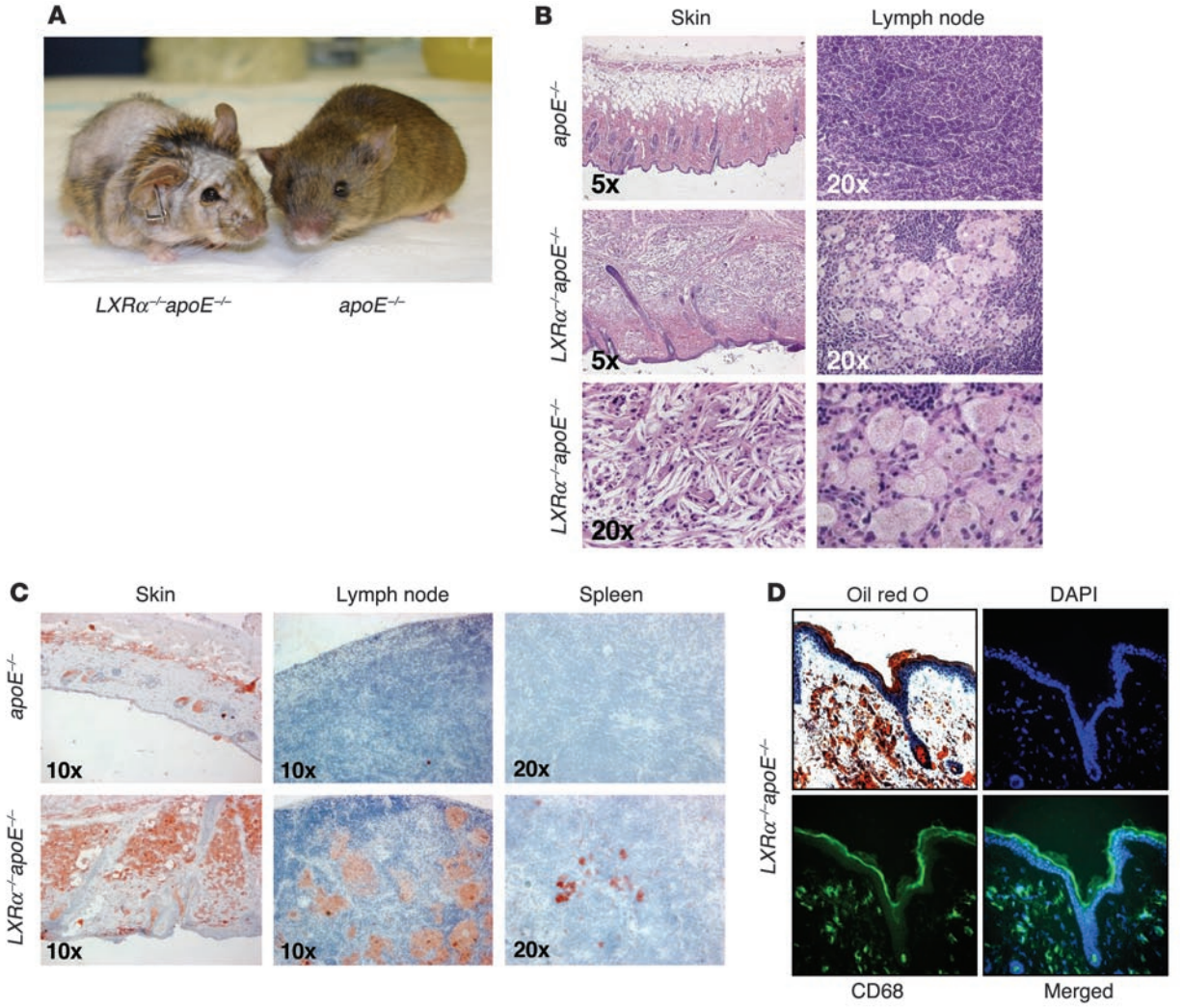

Figure 1
Accumulation of lipid in the peripheral tissues of *LXRα*$^{-/-}$*apoE*$^{-/-}$ mice. (**A**) *apoE*$^{-/-}$ and *LXRα*$^{-/-}$*apoE*$^{-/-}$ mice at 34 weeks of age; the double-knockout mouse exhibits marked skin thickening and alopecia. (**B** and **C**) Histological analysis of tissues from representative *apoE*$^{-/-}$ and *LXRα*$^{-/-}$*apoE*$^{-/-}$ mice at 34 weeks of age. There was increased lipid accumulation in the tissues from the double-knockout mice as revealed by H&E (**B**) and oil red O (**C**) staining. Original magnification is as indicated. (**D**) Lipid accumulation in the skin occurs primarily in macrophages as revealed by oil red O and CD68 costaining.

previous studies addressing the role of the LXRs in atherogenesis have focused solely on the consequence of loss of both LXRα and LXRβ. As a result, the specific roles of individual LXRs in whole-body cholesterol metabolism and atherosclerosis remain unclear. The question of whether LXRα and LXRβ have similar roles in the context of atherosclerosis is particularly important, since current strategies for LXR-targeted antiatherogenic drugs are focused on the development of LXRβ-selective ligands (23, 24). The rationale for this approach is the hypothesis that LXRα and LXRβ are equally effective in promoting cholesterol efflux in macrophages, while LXRα is the primary isotype responsible for the undesirable effects of LXR agonist on plasma triglyceride levels (7, 22, 25). Using *LXRα* single-knockout animals, both Quinet et al. and Lund et al. demonstrated that activation of LXRβ with an LXRα/β dual agonist can stimulate cholesterol efflux and increase HDL-cholesterol levels in mice without raising triglyceride levels (23, 24). However, whether selective activation of LXRβ impacts the development of cardiovascular disease remains unclear.

We demonstrate here that the LXRα isotype plays a critical role in maintaining whole-body cholesterol homeostasis in the context of hypercholesterolemia. Unexpectedly, mice lacking both LXRα and apoE (*LXRα*$^{-/-}$*apoE*$^{-/-}$ mice) exhibited massive cholesterol accumulation in peripheral tissues, increased whole-body cholesterol burden, and accelerated atherosclerosis. We further show that a highly efficacious synthetic agonist is able to compensate for the loss of LXRα and reduce atherosclerosis in *LXRα*$^{-/-}$*apoE*$^{-/-}$ mice, providing in vivo validation for the pursuit of LXRβ-specific ligands for the treatment of atherosclerosis.

Results

LXRα$^{-/-}$*apoE*$^{-/-}$ *mice exhibit extreme cholesterol accumulation in peripheral tissues*. To investigate the specific role of LXRα in whole-body

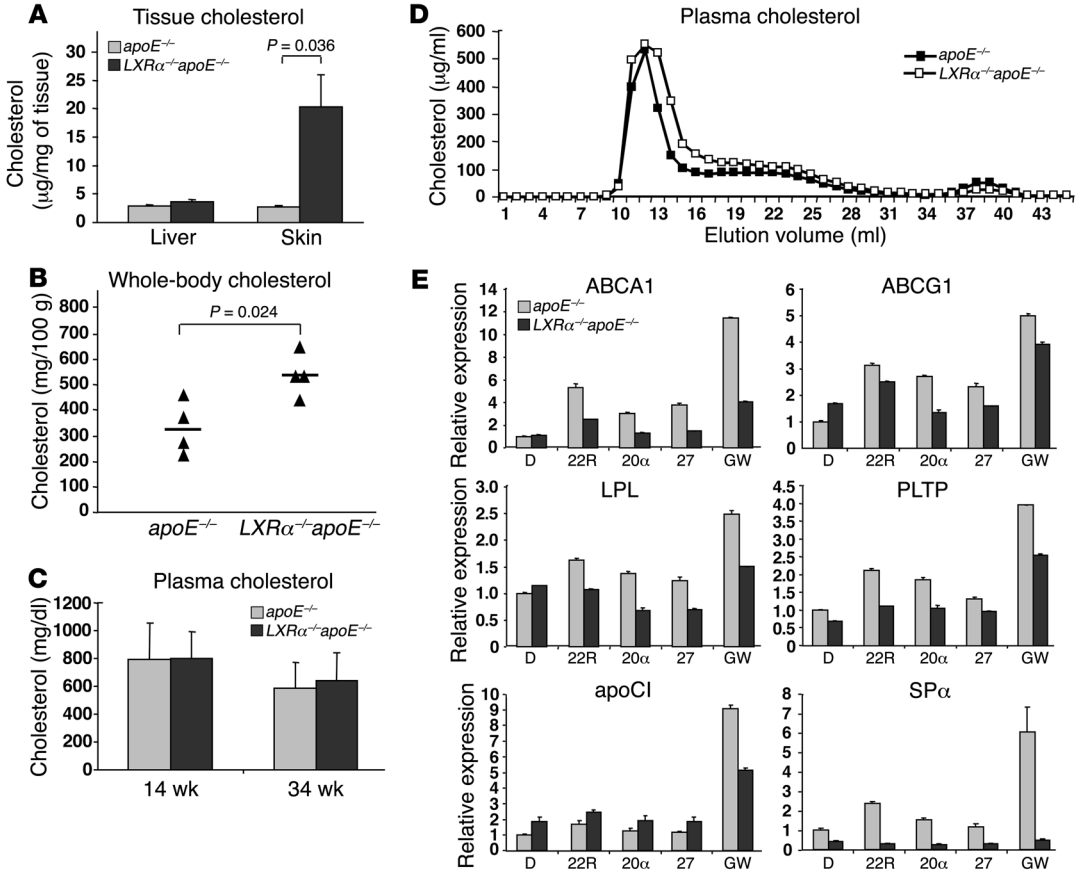

Figure 2

Quantification of cholesterol levels in tissue, whole mouse, and plasma. (**A**) Total liver and skin cholesterol levels of *apoE*$^{-/-}$ and *LXRα*$^{-/-}$*apoE*$^{-/-}$ mice at 34 weeks of age. Data are expressed as mean ± SEM. $n = 5$ per group. P value is indicated. (**B**) Whole-body cholesterol levels of *apoE*$^{-/-}$ or *LXRα*$^{-/-}$*apoE*$^{-/-}$ mice at 25 weeks of age. $n = 4$ per group. P value is indicated. (**C**) Total plasma cholesterol levels of *apoE*$^{-/-}$ or *LXRα*$^{-/-}$*apoE*$^{-/-}$ mice at 14 and 34 weeks of age. Data are expressed as mean ± SEM. $n = 9$–15 per group. (**D**) Fast protein liquid chromatography (FPLC) analysis of plasma cholesterol content of *apoE*$^{-/-}$ or *LXRα*$^{-/-}$*apoE*$^{-/-}$ mice at 14 weeks of age. Fasting plasma samples from 5 mice of each genotype were pooled for this analysis. (**E**) Expression of LXR target genes in peritoneal macrophages isolated from *apoE*$^{-/-}$ or *LXRα*$^{-/-}$*apoE*$^{-/-}$ mice. DMSO (D), 22(R)-, 20α-, and 27-hydroxycholesterol were used at 3 μM, and GW3965 (GW) was used at 1 μM. PLTP, phospholipid transfer protein.

cholesterol homeostasis and atherosclerosis, we generated mice that lack expression of both LXRα and apoE (*LXRα*$^{-/-}$*apoE*$^{-/-}$ mice). apoE-deficient mice develop spontaneous hyperlipidemia and provide a widely utilized model for atherosclerosis. We chose to disrupt LXRα expression so that ligand studies focused on targeting endogenous LXRβ could be undertaken (see below). Unexpectedly, although LXRα and LXRβ have been reported to compensate for one another in macrophages in mice with normal plasma cholesterol levels, we found that LXRβ cannot adequately compensate for the loss of LXRα in the context of the hypercholesterolemic *apoE*$^{-/-}$ background. As the *LXRα*$^{-/-}$*apoE*$^{-/-}$ mice aged, they exhibited marked skin thickening and alopecia compared with control *apoE*$^{-/-}$ mice (Figure 1A). The thickened skin was located predominately on the neck, limbs, and abdomen of all mice, although the extent of thickening and alopecia varied. Similar to that of other animal models of hypercholesterolemia (26–29), this phenotype is due in large measure to extreme accumulation of lipid within the skin. Lipid accumulation in *LXRα*$^{-/-}$*apoE*$^{-/-}$ mice was apparent in both H&E- and oil red O–stained sections (Figure 1, B and C). Furthermore, the skin of *LXRα*$^{-/-}$*apoE*$^{-/-}$ mice displayed an expanded dermis that was infiltrated with lipid-laden macrophages and cholesterol crystals. Confirmation that the intracellular lipid was located primarily within dermal macrophages was obtained by staining skin sections with the macrophage surface antigen CD68 (Figure 1D). In addition to skin, lipid accumulation in macrophages was also observed in other peripheral organs from *LXRα*$^{-/-}$*apoE*$^{-/-}$ mice, such as the lymph nodes and spleen (Figure 1, B and C). It is important to note that these phenotypes of alopecia, skin thickening, and foam cell accumulation were not observed in even very old (older than 1 year) wild-type or *LXRα*$^{-/-}$ mice (data not shown).

Quantification of tissue lipid levels demonstrated that the skin of the *LXRα*$^{-/-}$*apoE*$^{-/-}$ mice had dramatically increased total cholesterol content compared with that of *apoE*$^{-/-}$ controls (Figure 2A). Consistent with these observations, whole-body cholesterol levels in the *LXRα*$^{-/-}$*apoE*$^{-/-}$ mice were extraordinarily elevated (Figure 2B). In striking contrast to the tissue cholesterol levels, however, plasma cholesterol levels (Figure 2C) and fast protein liquid chromatography (FPLC) lipoprotein profiles (Figure 2D) did not differ not significantly between the genotypes.

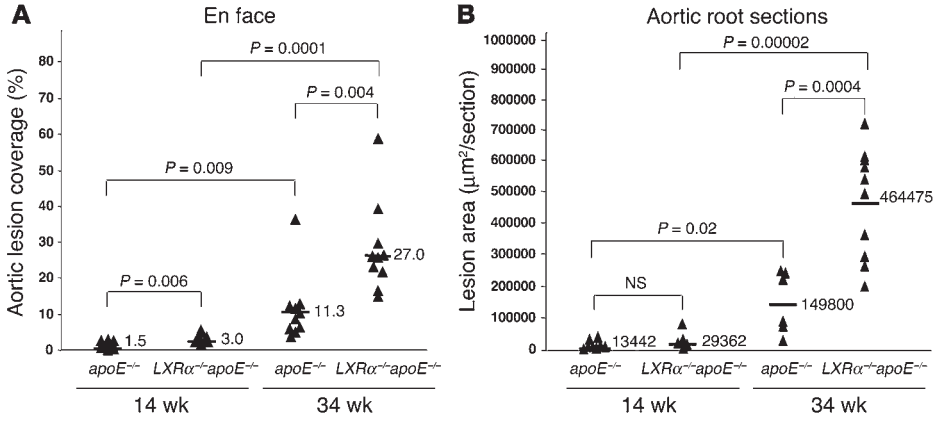

Figure 3
Accelerated atherosclerosis in *LXRα*$^{-/-}$*apoE*$^{-/-}$ mice at 14 and 34 weeks of age. (**A**) Analysis of atherosclerotic lesions of *apoE*$^{-/-}$ or *LXRα*$^{-/-}$*apoE*$^{-/-}$ mice as quantitated by en face analysis. n = 10–13 per group. (**B**) Analysis of aortic root lesions. n = 5–10 per group. P values are indicated. Horizontal lines indicate mean values.

LXRα and LXRβ are known to participate in reverse cholesterol transport by promoting cholesterol efflux from macrophages through the expression of genes such as the transporters *Abca1* and *Abcg1*. The above observations point to a potential defect in this pathway in *LXRα*$^{-/-}$*apoE*$^{-/-}$ mice. The phenotype of these mice suggests that cholesterol is not being properly effluxed from macrophages into the blood for return to the liver. Despite a marked accumulation of cholesterol in peripheral tissues, we did not observe significant defects in the expression of these transporters in the liver, lung, spleen, or skin in the *LXRα*$^{-/-}$*apoE*$^{-/-}$ mice compared with controls (data not shown). However, subtle defects in the expression of these transporters in macrophages within these organs may be difficult to detect, since macrophages constitute only a small percentage of cells in these organs. To further address this issue, we examined the expression of ABCA1 and ABCG1 in peritoneal macrophages isolated from *LXRα*$^{-/-}$*apoE*$^{-/-}$ and *apoE*$^{-/-}$ mice treated with endogenous or synthetic LXR ligands (Figure 2E). In all cases, we observed a fractional decrease in the ligand-mediated upregulation of these transporters in macrophages isolated from *LXRα*$^{-/-}$*apoE*$^{-/-}$ mice compared with controls. Defects in expression were also seen for additional LXR target genes involved in reverse cholesterol transport, including lipoprotein lipase (LPL) and the phospholipid transfer protein (PLTP). These results are consistent with previous studies that have reported gene dosage–dependent effects on the expression of some LXR target genes in isolated primary macrophages (30). Interestingly, in the absence of apoE, which is thought to be an important acceptor in ABCA1-mediated cholesterol efflux, other apolipoproteins in this gene cluster, such as apoCI, continue to be induced by ligand. As expected, SPα/AIM, an LXRα-specific target gene, was not regulated in macrophages isolated from *LXRα*$^{-/-}$*apoE*$^{-/-}$ mice.

LXRα$^{-/-}$*apoE*$^{-/-}$ *mice exhibit accelerated atherosclerosis.* The massive cholesterol accumulation observed in the peripheral tissues of the *LXRα*$^{-/-}$*apoE*$^{-/-}$ mice suggested that the loss of LXRα on this background might also lead to the accumulation of foam cells in the artery wall and exacerbated atherosclerosis. To quantify atherosclerosis development, en face lesion analysis was performed on aortas from mice at both 14 and 34 weeks of age. As expected, the extent of aortic lesion coverage in control mice increased with age (approximately 7.5-fold; Figure 3A). This was also observed in the *LXRα*$^{-/-}$*apoE*$^{-/-}$ mice, with aortic lesion coverage increasing approximately 9-fold. More importantly, the *LXRα*$^{-/-}$*apoE*$^{-/-}$ mice exhibited a 2-fold increase in atherosclerotic lesions throughout the aorta compared with control mice at 14 weeks of age and a 2.4-fold increase at 34 weeks of age. Similar results were obtained when atherosclerosis in these mice was assessed by quantification of oil red O–stained aortic root sections (Figure 3B). Although there was a 2-fold increase in lesion area in the *LXRα*$^{-/-}$*apoE*$^{-/-}$ mice compared with control mice at 14 weeks of age, this difference did not reach significance due to the small sample size for one of the genotypes. However, at 34 weeks of age, there was a highly significant, 3-fold increase in lesion area in the *LXRα*$^{-/-}$*apoE*$^{-/-}$ mice compared with controls. The above results clearly demonstrate that in the genetic absence of LXRα, the level of LXR pathway

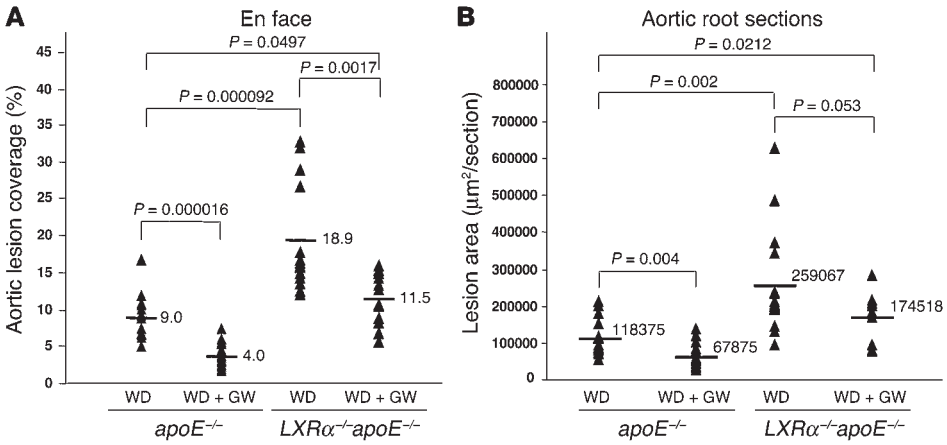

Figure 4
Treatment of *apoE*$^{-/-}$ and *LXRα*$^{-/-}$*apoE*$^{-/-}$ mice with synthetic LXR ligand reduces atherosclerosis. All mice were 14 weeks of age and were fed a Western diet (WD) with or without GW3965 for 11 weeks. (**A**) Analysis of atherosclerotic lesions as quantitated by en face analysis. n = 14–15 per group. (**B**) Analysis of aortic root lesions. n = 14–15 per group. P values are indicated. Horizontal lines indicate mean values.

Table 1
Plasma lipid levels of 14-week-old *apoE*$^{-/-}$ and *LXR*α$^{-/-}$*apoE*$^{-/-}$ mice maintained for 11 weeks on a Western diet in the presence or absence of GW3965

	apoE$^{-/-}$		*LXR*$^{-/-}$*apoE*$^{-/-}$	
	WD	WD + GW	WD	WD + GW
Total cholesterol, mg/dl	1,739.8 ± 93.9	1,235.8 ± 95.0[A]	1,721.1 ± 151.6	1,293.8 ± 88.5[B]
HDL cholesterol, mg/dl	20.8 ± 1.2	31.3 ± 2.4[A]	21.4 ± 1.6	29.2 ± 2.0[A]
Unesterified cholesterol, mg/dl	675.9 ± 34.6	425 ± 34.7[A]	612.9 ± 64.8	456.7 ± 31.1[B]

Data are expressed as mean ± SEM. [A]$P < 0.005$. [B]$P < 0.05$. n = 15–18 per group. GW, GW3965; WD, Western diet.

activation achieved by LXRβ and endogenous ligand is unable to maintain homeostasis in the setting of the apoE-null background. Moreover, the increased atherosclerosis in these mice is consistent with an inability of macrophages to efficiently efflux cholesterol through the LXR pathway. It is also important to note that whole-body cholesterol burden, but not plasma cholesterol levels, correlated with extent of atherosclerosis in the *LXR*α$^{-/-}$*apoE*$^{-/-}$ mice (Figure 2B and Figure 3A).

*Ligand activation of LXR*β *reduces atherosclerosis in LXR*α$^{-/-}$*apoE*$^{-/-}$ *mice.* Although endogenous ligand acting on LXRβ was unable to provide sufficient efflux activity to maintain homeostasis in *LXR*α$^{-/-}$*apoE*$^{-/-}$ mice, we asked whether a highly efficacious synthetic LXR agonist could alleviate cholesterol overload and provide antiatherogenic effects in this setting. This is a particularly important question, since current strategies for LXR-targeted antiatherogenic drugs are focused on the development of LXRβ-selective ligands (23, 24). Analysis of gene expression in peritoneal macrophages confirmed that the synthetic LXR agonist GW3965 was more efficacious than the endogenous activators 22(R)-hydroxycholesterol, 20α-hydroxycholesterol, and 27-hydroxycholesterol with respect to induction of LXR target genes (Figure 2E). To evaluate the activity of GW3965 in vivo, control and *LXR*α$^{-/-}$*apoE*$^{-/-}$ mice were placed on a Western diet or Western diet supplemented with GW3965 (20 mg/kg/d) from the time they were weaned (3 weeks old) until they were sacrificed. En face analysis was performed to quantify atherosclerosis development in mice that were fed Western diet with or without LXR ligand. Consistent with the results obtained on the normal chow diet (Figure 3), *LXR*α$^{-/-}$*apoE*$^{-/-}$ mice fed a Western diet exhibited a 2-fold increase in atherosclerotic lesion area throughout the aorta compared with *apoE*$^{-/-}$ control mice (Figure 4A). Importantly, GW3965 administration significantly inhibited the development of atherosclerotic lesions in both the *apoE*$^{-/-}$ and *LXR*α$^{-/-}$*apoE*$^{-/-}$ mice (by 56% and 39%, respectively), indicating that targeting LXRβ with GW3965 is able to compensate for the loss of LXRα and reduce atherosclerosis in *LXR*α$^{-/-}$*apoE*$^{-/-}$ mice. Comparable results were obtained when atherosclerosis in these mice was assessed by quantification of oil red O–stained aortic root sections (Figure 4B). Again, significant decreases in lesion area were observed in both *apoE*$^{-/-}$ and *LXR*α$^{-/-}$*apoE*$^{-/-}$ mice treated with LXR ligand (43% and 33% reduction, respectively). Consistent with previous studies, GW3965 treatment resulted in a decrease in total and unesterified cholesterol levels and an increase in HDL-cholesterol levels in both genotypes (Table 1). Additionally, although ligand administration resulted in a significant increase in plasma triglyceride levels in *apoE*$^{-/-}$ control mice, no significant effect was observed in the absence of LXRα (Figure 5, A and B). These observations provide the first evidence to our knowledge that pharmacologic activation of LXRβ alone can inhibit the development of atherosclerosis.

*Ligand activation of LXR*β *reverses cholesterol overload and decreases inflammation.* The observation that atherosclerosis was significantly reversed by GW3965 led us to ask whether this correlated with changes in whole-body cholesterol levels. Consistent with the results obtained with mice fed a normal chow diet, there was a dramatic (~2.5-fold) increase in whole-body cholesterol burden in *LXR*α$^{-/-}$*apoE*$^{-/-}$ mice on a Western diet compared with *apoE*$^{-/-}$ controls (Figure 6A). Furthermore, administration of the synthetic LXR ligand led to a comparable reduction in whole-body cholesterol levels in both *apoE*$^{-/-}$ mice and *LXR*α$^{-/-}$*apoE*$^{-/-}$ mice (although the reduction in the latter group did not achieve statistical significance). As the dramatic skin phenotype of *LXR*α$^{-/-}$*apoE*$^{-/-}$ mice (Figure 1) does not become apparent until later than the 14-week time point chosen for the atherosclerosis studies, it was not pos-

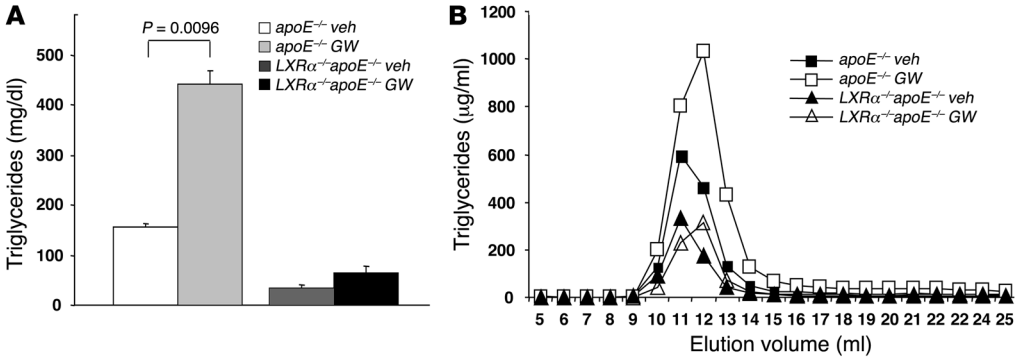

Figure 5
Triglyceride levels in *apoE*$^{-/-}$ and *LXR*α$^{-/-}$*apoE*$^{-/-}$ mice treated with synthetic LXR ligand. Mice were gavaged with either vehicle (Veh) or GW3965 (GW) once a day for 3 days. (**A**) Plasma triglyceride levels were determined for individual mice using an enzymatic assay. Data are expressed as mean ± SEM. n = 4 per group. P value is indicated. (**B**) Plasma samples were pooled, and FPLC analysis was conducted. n = 4 per group.

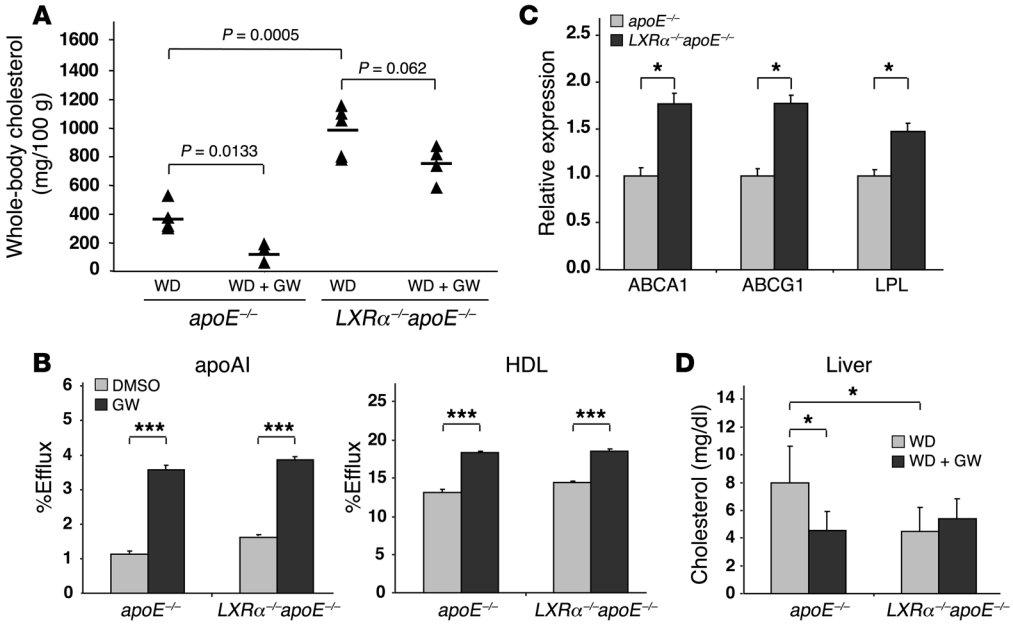

Figure 6
Treatment of *apoE*$^{-/-}$ and *LXRα*$^{-/-}$*apoE*$^{-/-}$ mice with synthetic LXR ligand ameliorates the cholesterol overload phenotype. (**A**) Whole-body cholesterol levels of *apoE*$^{-/-}$ or *LXRα*$^{-/-}$*apoE*$^{-/-}$ mice at 25 weeks of age that have been fed a Western diet with or without GW3965 for 22 weeks. $n = 3–5$ per group. *P* values are indicated. (**B**) apoAI- and HDL-specific cholesterol efflux from peritoneal macrophages isolated from *apoE*$^{-/-}$ or *LXRα*$^{-/-}$*apoE*$^{-/-}$ mice and treated with DMSO or GW3965. Experiments were conducted in quadruplicate. Data are expressed as mean ± SEM. ***$P < 0.0005$. (**C**) Basal gene expression in peritoneal macrophages isolated from mice fed a Western diet for 10 days. Data are expressed as mean ± SEM. $n = 3$ per group. *$P < 0.05$. (**D**) Total liver cholesterol levels of *apoE*$^{-/-}$ or *LXRα*$^{-/-}$*apoE*$^{-/-}$ mice fed a Western diet with or without GW3965. Data are expressed as mean ± SEM. $n = 5–8$ per group. *$P < 0.05$.

sible to determine whether this phenotype was reversed by LXR agonist. However, since a very large fraction of excess cholesterol accumulates in skin (Figure 2A), and since whole-body cholesterol burden was reduced by agonist, it is very likely that cholesterol accumulation in skin was reduced in agonist-treated mice.

To address whether ligand administration was alleviating cholesterol overload by inducing reverse cholesterol transport, we performed efflux assays. GW3965 was capable of inducing apoAI- and HDL-specific efflux in peritoneal macrophages from both *LXRα*$^{-/-}$*apoE*$^{-/-}$ mice and *apoE*$^{-/-}$ controls, which may partially explain the antiatherogenic effects of ligand treatment (Figure 6B). Despite the fractional decrease in the expression of genes involved in reverse cholesterol transport observed in response to synthetic agonist, in vitro efflux assays did not demonstrate a functional difference between genotypes. However, the sensitivity of this assay is very low, with only a 2- to 3-fold increase in efflux observed with synthetic LXR agonist. Clearly, *LXRα*$^{-/-}$*apoE*$^{-/-}$ macrophages in vivo have a marked defect in efflux, because they accumulate more cholesterol than *apoE*$^{-/-}$ controls in the face of similar plasma cholesterol levels.

Analysis of basal LXR target gene expression in freshly isolated peritoneal macrophages from Western diet–fed mice also supported a cholesterol efflux defect in *LXRα*$^{-/-}$*apoE*$^{-/-}$macrophages. Basal expression of *Abca1*, *Abcg1*, and *Lpl* was modestly but significantly higher in *LXRα*$^{-/-}$*apoE*$^{-/-}$ cells compared with *apoE*$^{-/-}$ controls, consistent with the chronic accumulation of elevated levels of oxysterol LXR activators within these cells (Figure 6C). This compensatory increase in LXR target gene expression in cells with defects in the cholesterol efflux pathway is similar to that recently observed in *Abcg1*$^{-/-}$ macrophages in vivo (31, 32). In the setting of short-term oxysterol ligand treatment, *apoE*$^{-/-}$ cells are more responsive to ligand than *LXRα*$^{-/-}$*apoE*$^{-/-}$ cells (Figure 2E). In the face of chronic hypercholesterolemia, however, *apoE*$^{-/-}$ macrophages are able to maintain cholesterol homeostasis and clear the excess cholesterol through the LXR pathway, whereas cholesterol slowly builds up in *LXRα*$^{-/-}$*apoE*$^{-/-}$ cells and the level of LXR target gene activation by endogenous ligand is unable to keep up with this burden.

The increase in reverse cholesterol transport of cholesterol from the periphery to the liver in *LXRα*$^{-/-}$*apoE*$^{-/-}$ mice treated with GW3965 did not result in an increase in hepatic cholesterol content (Figure 6D), indicating that the ability to remove cholesterol from the body is preserved in ligand-treated *LXRα*$^{-/-}$*apoE*$^{-/-}$ mice. Although formal studies of cholesterol secretion were not performed, gene expression studies indicated that basal expression of hepatic ABCA1, ABCG5, ABCG8, and CYP7A1 was not defective in *LXRα*$^{-/-}$*apoE*$^{-/-}$ mice compared with *apoE*$^{-/-}$ mice (Figure 7A). Consistent with previous work, synthetic LXR agonist failed to induce expression of *Abca1*, *Abcg1*, and *Cyp7a1* in the *LXRα*$^{-/-}$*apoE*$^{-/-}$ mice (24, 33). The preserved response of ABCA1 to ligand is likely due to the prominent expression of this gene in Kupffer cells, which, in contrast to hepatocytes, express high levels of both LXRα and LXRβ. As expected, expression of the LXRα-selective target gene SPα was severely compromised in *LXRα*$^{-/-}$*apoE*$^{-/-}$ mice. It is also worth noting that the *LXRα*$^{-/-}$*apoE*$^{-/-}$ mice did not show a compensatory increase in hepatic or intestinal expression of LXRβ (Figure 7, A and B).

Previous studies have demonstrated that LXR activation decreases intestinal absorption of cholesterol through the induction of

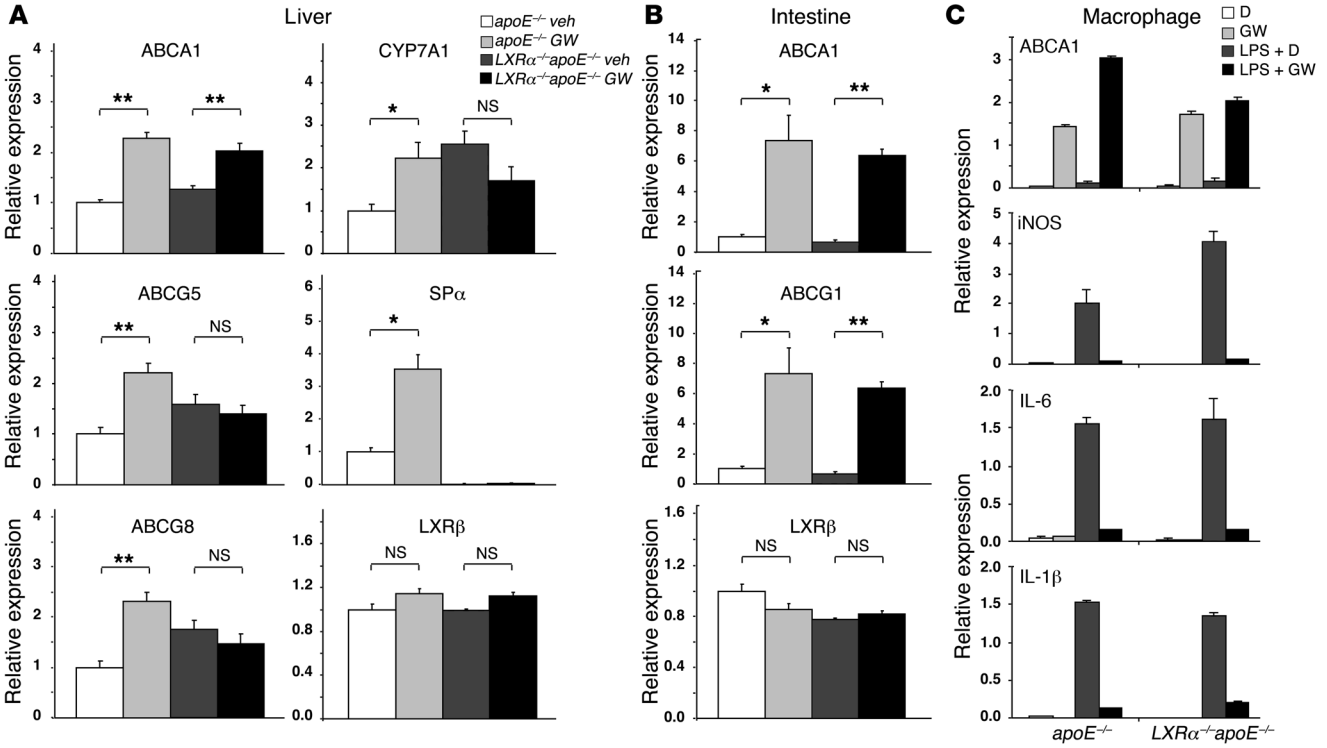

Figure 7

Gene expression in the liver, intestine, and peritoneal macrophages from *apoE*$^{-/-}$ or *LXRα*$^{-/-}$*apoE*$^{-/-}$ mice. (**A** and **B**) Mice were gavaged with either vehicle or GW3965 once a day for 3 days. Liver (**A**) and intestine (**B**) RNA was isolated, and real-time PCR was conducted for the listed genes. Data are expressed as mean ± SEM. $n = 4$ per group. $^{*}P < 0.05$; $^{**}P < 0.005$. (**C**) Peritoneal macrophages were treated with DMSO or GW3965 in the presence or absence of LPS. RNA was isolated, and real-time PCR was conducted for the listed genes.

ABC transporters (11, 33). Recent studies have also indicated that the intestine may play a role as an excretory organ in reverse cholesterol transport (34, 35). In contrast to those in the liver, where loss of LXRα expression compromises response to LXR agonist, target genes in the intestine were highly responsive to synthetic ligand in both *apoE*$^{-/-}$ and *LXRα*$^{-/-}$*apoE*$^{-/-}$ mice (Figure 7B). This observation, coupled with the fact that treatment with LXR agonist led to a decrease in plasma cholesterol levels in both genotypes (Table 1), strongly suggests that the intestine may be an important contributor to the therapeutic effects of agonist in *LXRα*$^{-/-}$*apoE*$^{-/-}$ mice.

Previous work has also demonstrated that LXR ligands negatively regulate inflammatory gene expression (14). To determine whether LXRβ alone is capable of reducing cytokine production in the absence of apoE, peritoneal macrophages from *LXRα*$^{-/-}$*apoE*$^{-/-}$ and control mice were treated with LPS in the presence or absence of GW3965. Consistent with previous results, ligand activation of LXRβ efficiently inhibited the expression of *iNOS*, *IL6*, and *IL1B* (Figure 7C). Thus, it is possible that decreases in inflammatory gene expression mediated by LXRβ may also contribute to the reduction in atherosclerosis observed in *LXRα*$^{-/-}$*apoE*$^{-/-}$ and control mice treated with the synthetic LXR agonist.

Discussion

The relative importance of the 2 LXRs in atherosclerosis susceptibility and treatment has not to our knowledge been addressed previously. Prior in vivo studies of the role of LXRs in cardiovascular disease have focused solely on mice or cells lacking both LXRα and LXRβ. Consequently, the question of whether LXRα and LXRβ have nonredundant roles in the control of the macrophage cholesterol efflux pathway and foam cell formation in the context of hypercholesterolemia have remained unclear. We have shown here that LXRα is essential for maintenance of whole-body cholesterol homeostasis and peripheral cholesterol efflux in the context of the hypercholesterolemic *apoE*$^{-/-}$ background. Mice lacking both LXRα and apoE display massive cholesterol accumulation in peripheral tissues, increased whole-body cholesterol burden, and accelerated atherosclerosis. Intriguingly, whole-body cholesterol levels, which are normally very tightly regulated, were increased by more than 100% in the *LXRα*$^{-/-}$*apoE*$^{-/-}$ mice. Moreover, this increased whole-body cholesterol burden correlated closely with increased susceptibility to atherosclerosis. These observations strongly suggest that while the activity of a single LXR is sufficient to maintain homeostasis when plasma cholesterol levels are low, the activity of both LXRα and LXRβ is essential for the ability to respond to the challenge of hypercholesterolemia.

Interestingly, the phenotype of the *LXRα*$^{-/-}$*apoE*$^{-/-}$ mice differs markedly from that of the *LXRα*$^{-/-}$ mice fed a cholesterol-rich diet (22). *LXRα*$^{-/-}$ mice fed a cholesterol-rich diet accumulate large amounts of cholesterol in the liver and rapidly develop hepatic failure. This phenotype is due in part to the inability of *LXRα*$^{-/-}$ mice to induce the expression of the rate-limiting enzyme in bile acid synthesis, CYP7A1. In *LXRα*$^{-/-}$ mice, cholesterol does not accumulate in the peripheral tissues, presumably because it is removed by the reverse cholesterol transport pathway and

returned to the liver. We postulate that the activity of LXRβ is sufficient to activate macrophage target gene expression and promote effective cholesterol efflux in *LXRα*$^{-/-}$ mice (22). By contrast, the phenotypes of the *LXRα*$^{-/-}$*apoE*$^{-/-}$ mice are consistent with defects in the cellular cholesterol efflux and reverse cholesterol transport pathways. Ablation of apoE expression impairs the ability of apoE-containing lipoproteins to be taken up by the liver, and this likely explains why hepatic cholesterol content was not different in *apoE*$^{-/-}$ and *LXRα*$^{-/-}$*apoE*$^{-/-}$ mice. At the same time, the apoE mutation presents the challenge of severe hypercholesterolemia to peripheral tissues. In *LXRα*$^{-/-}$*apoE*$^{-/-}$ mice, it appears that the activity of LXRβ on the efflux pathway is not sufficient to handle the massive cholesterol burden, despite the presence of endogenous ligands. Cholesterol is not efficiently transferred to HDL and returned to the liver, so the majority of the cholesterol is retained in macrophages within peripheral tissues.

We have considered the possibility that there may be LXRα-specific target genes whose protein products provide specific antiatherogenic effects, and this possibility cannot be entirely excluded. However, the observation that ligand activation of LXRβ can ameliorate the enhanced atherosclerosis seen in *LXRα*$^{-/-}$*apoE*$^{-/-}$ mice argues against this interpretation. The fact that pharmacologic activation of LXRβ can overcome the deficit in LXRα activity suggests that the relevant target genes involved must respond to both receptors. Quantitatively decreased expression of LXR target genes such as ABCA1, ABCG1, LPL, and PLTP, which are known to be involved in reverse cholesterol transport, provides a straightforward explanation for the accumulation of cholesterol in the peripheral tissues of *LXRα*$^{-/-}$*apoE*$^{-/-}$ mice. An alternative possibility is that the combined loss of apoE and LXRα expression in macrophages has a synergistic inhibitory effect on cholesterol efflux. The apoE gene is itself a direct target for LXR in macrophages and has been proposed to have an important role in cellular cholesterol efflux (30). apoE can serve as an acceptor for effluxed cholesterol and may also be involved in intracellular cholesterol trafficking (36–40). The observation that basal expression of LXR target genes is modestly elevated in macrophages from *LXRα*$^{-/-}$*apoE*$^{-/-}$ mice maintained on a Western diet is consistent with a defect in the efflux pathway. Interestingly, similar compensatory changes are observed in macrophages lacking the LXR target gene ABCG1 (31, 32). In the future, it will be of interest to determine whether combined loss of LXRβ and apoE or of LXRs and the LDL receptor in mice lead to similar phenotypes.

The ability of the LXRs to induce macrophage cholesterol efflux and to inhibit inflammatory gene expression has generated widespread interest in these proteins as potential targets for atherosclerosis therapy. Although synthetic LXR ligands have been shown to have beneficial effects on atherosclerosis development in mice, these agents also increase triglyceride levels, which are an independent risk factor for atherosclerosis. LXRα is the predominant LXR expressed in liver, and the ability of LXR agonist to stimulate hepatic lipogenesis is thought to result primarily from LXRα regulation of SREBP1c and Fas expression (41–43). The relative importance of LXRα in the liver has stimulated an interest in the development of LXRβ-selective agonists as potential atherosclerosis therapeutics. However, the question of whether activation of the LXRβ pathway is sufficient to reduce atherosclerosis has not been addressed. We have demonstrated here that the nonselective synthetic agonist GW3965 is able to reduce whole-body cholesterol levels and atherosclerosis in *LXRα*$^{-/-}$*apoE*$^{-/-}$ mice through the targeting of LXRβ. Clearly, the increased potency of the synthetic ligand compared with endogenous ligand provided sufficient LXRβ activation to compensate for the loss of LXRα. Importantly, this occurred without an increase in plasma triglyceride levels. Although GW3965 did not completely reduce disease burden to a level comparable to that in *apoE*$^{-/-}$ mice (Figure 4), it is possible that maximal LXRβ agonism may require a higher dose of ligand. Alternatively, as discussed above, it is also possible that there may be some LXRα-specific effects that cannot be compensated for by LXRβ. Finally, it is also possible that this simply reflects the fact that mice were only treated with agonist for part of their life (from 3 to 14 weeks of age). Perhaps treatment from birth would have led to further reductions in lesion formation. Nevertheless, the results presented here provide strong support for LXRβ as a potential target for the treatment of atherosclerosis.

Methods

Reagents. The synthetic LXR ligand GW3965 was provided by T. Willson (GlaxoSmithKline). 22(R)- and 20α-hydroxycholesterol were from Sigma-Aldrich and 27-hydroxycholesterol was from Research Plus. apoAI and HDL were from Intracel.

Animals and diets. All animals (Sv129 and C57BL/6 background) were housed in a temperature-controlled room under a 12-hour light/12-hour dark cycle and under pathogen-free conditions. *LXRα*$^{-/-}$ mice were originally provided by David Mangelsdorf, University of Texas Southwestern Medical Center, Dallas, Texas, USA. *apoE*$^{-/-}$ mice were from The Jackson Laboratory. Males were used in all experiments and were fed either standard chow, Western diet (21% fat, 0.21% cholesterol; D12079B; Research Diets Inc.), or Western diet supplemented so that mice received 20 mg/kg/d of GW3965, as indicated. For the set of mice that were placed on a Western diet with or without GW3965, this was done from the time they were weaned (3 weeks old) until they were sacrificed. For gavage experiments, mice were gavaged with either vehicle or 20 mg/kg of GW3965 once a day for 3 days. Tissues and blood were harvested 4 hours after the last gavage. All animal experiments were approved by the Institutional Animal Care and Research Advisory Committee of the UCLA.

Whole-body cholesterol analysis. Analysis was conducted as previously described (29). Briefly, after a mouse was euthanized, the gastrointestinal (GI) tract was removed and the contents were washed out. Each mouse and cleaned GI tract was placed in a 250-ml Pyrex beaker containing 10 g KOH and 150 ml ethanol. The beaker was covered with aluminum foil, and the carcass was allowed to autodigest for 4 days at room temperature. The contents of the beaker were then stirred on a hot plate until the ethanol volume decreased to 50 ml. The contents were filtered into a 100-ml volumetric flask using 2 layers of stretched gauze over a glass funnel. The flask was allowed to cool, and the volume was adjusted to 100 ml with ethanol. The flask was inverted to mix the contents evenly, and the cholesterol content was determined using a commercially available enzymatic kit (Sigma-Aldrich). Data are expressed as milligrams of cholesterol per 100 grams of body weight.

Tissue and plasma lipid analysis. Lipids were extracted from tissues using the Folch method (44, 45). Briefly, chloroform extracts were dried under nitrogen and resolubilized in water. Cholesterol content was determined using a commercially available enzymatic kit (Sigma-Aldrich). Data are expressed as milligrams of cholesterol per gram of tissue weight. For plasma lipid analysis, mice were fasted overnight and euthanized. Blood was collected from the abdominal vena cava. Aliquots of plasma were analyzed for cholesterol content as described previously (17). Plasma lipoproteins that were fractionated using an FPLC system were processed as previously described (46).

Histological and lesion analysis. Immunohistochemistry of skin sections and preparation and staining of frozen and paraffin-embedded sections from

tissues were performed as described previously (47, 48). Atherosclerosis in the aortic roots and the descending aortas (en face) were quantified by computer-assisted image analysis as described (49). Atherosclerotic lesions at the aortic valve were analyzed as described (50). Comparisons between groups were made using the Student's *t* test for independent samples (2 tailed). *P* less than 0.05 was considered significant.

RNA isolation and analysis. Total RNA was isolated from tissues using TRIzol (Invitrogen). One microgram of total RNA was reverse transcribed with random hexamers using the Taqman Reverse Transcription Reagents Kit (Applied Biosystems). Sybergreen (Diagenode) real-time quantitative PCR assays were performed using an Applied Biosystems 7900HT sequence detector. Results show averages of duplicate experiments normalized to 36B4. The primer sequences were as follows: ABCA1 forward, 5′-GGTTTGGAGATGGTTATACAATAGTTGT; ABCA1 reverse, 5′-CCCGGAAACGCAAGTCC; ABCG1 forward, 5′-TCACCCAGTTCTGCATCCTCTT; ABCG1 reverse, 5′-GCAGATGTGTCAGGACCGAGT; ABCG5 forward, 5′-TGGATCCAACACCTCTATGCTAAA; ABCG5 reverse, 5′-GGCAGGTTTTCTCGATGAACTG; ABCG8 forward, 5′-TGCCCACCTTCCACATGTC; ABCG8 reverse, 5′-ATGAAGCCGGCAGTAAGGTAGA; LPL forward, 5′-GTGGCCGAGAGCGAGAAC; LPL reverse, 5′-AAGAAGGAGTAGGTTTTATTTGTGGA; PLTP forward, 5′-GGAGGGTGTGTCCATCCGA; PLTP reverse, 5′-CCCCGAAGGCCATATTCATTTTA; apoCI forward, 5′-AAGGAGAAGTTGAAGACCACGTTC; apoCI reverse, 5′-GATGTCCTTGATGCTTCGAGG; Spα forward, 5′-TTTGTTGGATCGTGTTTTTCAGA; Spa reverse, 5′-CTTCACAGCGGTGGGCA; Cyp7a1 forward, 5′-AGCAACTAAACAACCTGCCAGTACTA; Cyp7a1 reverse, 5′-GTCCGGATATTCAAGGATGCA; LXRβ forward, 5′-CCCCACAAGTTCTCTGGACACT; LXRβ reverse, 5′-TGACGTGGCGGAGGTACTG; iNOS forward, 5′-GCAGCTGGGCTGTACAAA; iNOS reverse, 5′-AGCGTTTCGGGATCTGAAT; IL-6 forward, 5′-CTGCAAGAGACTTCCATCCAGTT; IL-6 reverse, 5′-GAAGTAGGGAAGGCCGTGG; IL-1β forward, 5′-AGAAGCTGTGGCAGCTACCTG; IL-1β reverse, 5′-GGAAAAGAAGGTGCTCATGTCC.

Peritoneal macrophages. Peritoneal macrophages were obtained from thioglycollate-treated mice 4 days after injection. For gene expression studies, cells were placed in DMEM plus 0.5% FBS plus 5 μM simvastatin plus 100 μM mevalonic acid overnight. Cells were then treated with DMSO or ligand for LXR as indicated for 24 hours. Total RNA was extracted and analyzed by real-time PCR. For cholesterol efflux assays, peritoneal cells were labeled with [^{3}H]cholesterol (1.0 μCi/ml) in the presence of acyl-CoA: cholestrol *O*-acyltransferase inhibitor (2 μg/ml) either with DMSO or with ligand for LXR (1 μM GW3965). After equilibrating the cholesterol pools, cells were washed with PBS and incubated in DMEM containing 0.2% BSA in the absence or presence of apoAI (15 μg/ml) or HDL (50 μg/ml) for 6 hours. Radioactivity in the medium and total cell-associated radioactivity was determined by scintillation counting. The assays were performed in quadruplicate and are presented as percentage apoAI- or HDL-specific efflux. For macrophage inflammatory responses, peritoneal cells were placed in DMEM plus 0.5% FBS plus 5 μM simvastatin plus 100 μM mevalonic acid overnight. Cells were then stimulated with DMSO or ligand for LXR (1 μM GW3965) for 24 hours. Cells were then treated with or without LPS (100 ng/ml) for 5 hours. Total RNA was extracted and analyzed by real-time PCR.

Acknowledgments

We thank David Mangelsdorf for the LXR-null mice and Tim Willson for GW3965. We are extremely grateful to Jon V. Salazar for his dedicated help with the mouse colony. P. Tontonoz is an investigator of the Howard Hughes Medical Institute. This work was supported by NIH Training Grants CA09056 and HL69766 (to M.N. Bradley) and grants HL66088 and HL30568 (to P. Tontonoz).

Received for publication February 21, 2007, and accepted in revised form May 17, 2007.

Address correspondence to: Peter Tontonoz, Howard Hughes Medical Institute, UCLA School of Medicine, Box 951662, Los Angeles, California 90095-1662, USA. Phone: (310) 206-4546; Fax: (310) 267-0382; E-mail: ptontonoz@mednet.ucla.edu.

1. Glass, C.K., and Witztum, J.L. 2001. Atherosclerosis: the road ahead. *Cell.* **104**:503–516.
2. Lusis, A.J. 2000. Atherosclerosis. *Nature.* **407**:233–241.
3. Janowski, B.A., Willy, P.J., Devi, T.R., Falck, J.R., and Mangelsdorf, D.J. 1996. An oxysterol signalling pathway mediated by the nuclear receptor LXR alpha. *Nature.* **383**:728–731.
4. Lehmann, J.M., et al. 1997. Activation of the nuclear receptor LXR by oxysterols defines a new hormone response pathway. *J. Biol. Chem.* **272**:3137–3140.
5. Fu, X., et al. 2001. 27-Hydroxycholesterol is an endogenous ligand for liver X receptor in cholesterol-loaded cells. *J. Biol. Chem.* **276**:38378–38387.
6. Collins, J.L., et al. 2002. Identification of a nonsteroidal liver X receptor agonist through parallel array synthesis of tertiary amines. *J. Med. Chem.* **45**:1963–1966.
7. Schultz, J.R., et al. 2000. Role of LXRs in control of lipogenesis. *Genes Dev.* **14**:2831–2838.
8. Zelcer, N., and Tontonoz, P. 2006. Liver X receptors as integrators of metabolic and inflammatory signaling. *J. Clin. Invest.* **116**:607–614. doi:10.1172/JCI27883.
9. Tontonoz, P., and Mangelsdorf, D.J. 2003. Liver X receptor signaling pathways in cardiovascular disease. *Mol. Endocrinol.* **17**:985–993.
10. Berge, K.E., et al. 2000. Accumulation of dietary cholesterol in sitosterolemia caused by mutations in adjacent ABC transporters. *Science.* **290**:1771–1775.
11. Repa, J.J., et al. 2000. Regulation of absorption and ABC1-mediated efflux of cholesterol by RXR heterodimers. *Science.* **289**:1524–1529.
12. Costet, P., Luo, Y., Wang, N., and Tall, A.R. 2000. Sterol-dependent transactivation of the ABC1 promoter by the liver X receptor/retinoid X receptor. *J. Biol. Chem.* **275**:28240–28245.
13. Schwartz, K., Lawn, R.M., and Wade, D.P. 2000. ABC1 gene expression and ApoA-I-mediated cholesterol efflux are regulated by LXR. *Biochem. Biophys. Res. Commun.* **274**:794–802.
14. Joseph, S.B., Castrillo, A., Laffitte, B.A., Mangelsdorf, D.J., and Tontonoz, P. 2003. Reciprocal regulation of inflammation and lipid metabolism by liver X receptors. *Nat. Med.* **9**:213–219.
15. Schuster, G.U., et al. 2002. Accumulation of foam cells in liver X receptor-deficient mice. *Circulation.* **106**:1147–1153.
16. Tangirala, R.K., et al. 2002. Identification of macrophage liver X receptors as inhibitors of atherosclerosis. *Proc. Natl. Acad. Sci. U. S. A.* **99**:11896–11901.
17. Joseph, S.B., et al. 2002. Synthetic LXR ligand inhibits the development of atherosclerosis in mice. *Proc. Natl. Acad. Sci. U. S. A.* **99**:7604–7609.
18. Levin, N., et al. 2005. Macrophage liver X receptor is required for antiatherogenic activity of LXR agonists. *Arterioscler. Thromb. Vasc. Biol.* **25**:135–142.
19. Terasaka, N., et al. 2003. T-0901317, a synthetic liver X receptor ligand, inhibits development of atherosclerosis in LDL receptor-deficient mice. *FEBS Lett.* **536**:6–11.
20. Mak, P.A., et al. 2002. Regulated expression of the apolipoprotein E/C-I/C-IV/C-II gene cluster in murine and human macrophages. A critical role for nuclear liver X receptors alpha and beta. *J. Biol. Chem.* **277**:31900–31908.
21. Venkateswaran, A., et al. 2000. Human white/murine ABC8 mRNA levels are highly induced in lipid-loaded macrophages. A transcriptional role for specific oxysterols. *J. Biol. Chem.* **275**:14700–14707.
22. Peet, D.J., et al. 1998. Cholesterol and bile acid metabolism are impaired in mice lacking the nuclear oxysterol receptor LXR alpha. *Cell.* **93**:693–704.
23. Lund, E.G., et al. 2006. Different roles of liver X receptor alpha and beta in lipid metabolism: effects of an alpha-selective and a dual agonist in mice deficient in each subtype. *Biochem. Pharmacol.* **71**:453–463.
24. Quinet, E.M., et al. 2006. Liver X receptor (LXR)-β regulation in LXRα-deficient mice: implications for therapeutic targeting. *Mol. Pharmacol.* **70**:1340–1349.
25. Alberti, S., et al. 2001. Hepatic cholesterol metabolism and resistance to dietary cholesterol in LXRβ-deficient mice. *J. Clin. Invest.* **107**:565–573.
26. Accad, M., et al. 2000. Massive xanthomatosis and altered composition of atherosclerotic lesions in hyperlipidemic mice lacking acyl CoA:cholesterol acyltransferase 1. *J. Clin. Invest.* **105**:711–719.
27. Ishibashi, S., Goldstein, J.L., Brown, M.S., Herz, J., and Burns, D.K. 1994. Massive xanthomatosis and atherosclerosis in cholesterol-fed low density lipoprotein receptor-negative mice. *J. Clin. Invest.* **93**:1885–1893.
28. Yagyu, H., et al. 2000. Absence of ACAT-1 attenuates atherosclerosis but causes dry eye and cutaneous xanthomatosis in mice with congenital hyperlipidemia. *J. Biol. Chem.* **275**:21324–21330.
29. Zabalawi, M., et al. 2007. Inflammation and skin cholesterol in LDLr$^{-/-}$, apoA-I$^{-/-}$ mice: link between

cholesterol homeostasis and self-tolerance? *J. Lipid Res.* **48**:52–65.
30. Laffitte, B.A., et al. 2001. LXRs control lipid-inducible expression of the apolipoprotein E gene in macrophages and adipocytes. *Proc. Natl. Acad. Sci. U. S. A.* **98**:507–512.
31. Baldan, A., et al. 2006. Deletion of the transmembrane transporter ABCG1 results in progressive pulmonary lipidosis. *J. Biol. Chem.* **281**:29401–29410.
32. Ranalletta, M., et al. 2006. Decreased atherosclerosis in low-density lipoprotein receptor knockout mice transplanted with Abcg1$^{-/-}$ bone marrow. *Arterioscler. Thromb. Vasc. Biol.* **26**:2308–2315.
33. Repa, J.J., et al. 2002. Regulation of ATP-binding cassette sterol transporters ABCG5 and ABCG8 by the liver X receptors alpha and beta. *J. Biol. Chem.* **277**:18793–18800.
34. Kruit, J.K., et al. 2005. Increased fecal neutral sterol loss upon liver X receptor activation is independent of biliary sterol secretion in mice. *Gastroenterology.* **128**:147–156.
35. Plosch, T., et al. 2002. Increased hepatobiliary and fecal cholesterol excretion upon activation of the liver X receptor is independent of ABCA1. *J. Biol. Chem.* **277**:33870–33877.
36. Hayek, T., Oiknine, J., Brook, J.G., and Aviram, M. 1994. Role of HDL apolipoprotein E in cellular cholesterol efflux: studies in apo E knockout transgenic mice. *Biochem. Biophys. Res. Commun.* **205**:1072–1078.
37. Krimbou, L., et al. 2004. Molecular interactions between apoE and ABCA1: impact on apoE lipidation. *J. Lipid Res.* **45**:839–848.
38. Mazzone, T. 1996. Apolipoprotein E secretion by macrophages: its potential physiological functions. *Curr. Opin. Lipidol.* **7**:303–307.
39. Zhang, W.Y., Gaynor, P.M., and Kruth, H.S. 1996. Apolipoprotein E produced by human monocyte-derived macrophages mediates cholesterol efflux that occurs in the absence of added cholesterol acceptors. *J. Biol. Chem.* **271**:28641–28646.
40. Langer, C., et al. 2000. Endogenous apolipoprotein E modulates cholesterol efflux and cholesteryl ester hydrolysis mediated by high-density lipoprotein-3 and lipid-free apolipoproteins in mouse peritoneal macrophages. *J. Mol. Med.* **78**:217–227.
41. Joseph, S.B., et al. 2002. Direct and indirect mechanisms for regulation of fatty acid synthase gene expression by liver X receptors. *J. Biol. Chem.* **277**:11019–11025.
42. Repa, J.J., et al. 2000. Regulation of mouse sterol regulatory element-binding protein-1c gene (SREBP-1c) by oxysterol receptors, LXRalpha and LXRbeta. *Genes Dev.* **14**:2819–2830.
43. Yoshikawa, T., et al. 2001. Identification of liver X receptor-retinoid X receptor as an activator of the sterol regulatory element-binding protein 1c gene promoter. *Mol. Cell. Biol.* **21**:2991–3000.
44. Folch, J., Lees, M., and Sloane Stanley, G.H. 1957. A simple method for the isolation and purification of total lipides from animal tissues. *J. Biol. Chem.* **226**:497–509.
45. Carr, T.P., Andresen, C.J., and Rudel, L.L. 1993. Enzymatic determination of triglyceride, free cholesterol, and total cholesterol in tissue lipid extracts. *Clin. Biochem.* **26**:39–42.
46. Hedrick, C.C., Castellani, L.W., Warden, C.H., Puppione, D.L., and Lusis, A.J. 1993. Influence of mouse apolipoprotein A-II on plasma lipoproteins in transgenic mice. *J. Biol. Chem.* **268**:20676–20682.
47. Arai, S., et al. 2005. A role for the apoptosis inhibitory factor AIM/Spalpha/Api6 in atherosclerosis development. *Cell Metab.* **1**:201–213.
48. Kennedy, M.A., et al. 2005. ABCG1 has a critical role in mediating cholesterol efflux to HDL and preventing cellular lipid accumulation. *Cell Metab.* **1**:121–131.
49. Tangirala, R.K., Rubin, E.M., and Palinski, W. 1995. Quantitation of atherosclerosis in murine models: correlation between lesions in the aortic origin and in the entire aorta, and differences in the extent of lesions between sexes in LDL receptor-deficient and apolipoprotein E-deficient mice. *J. Lipid Res.* **36**:2320–2328.
50. Shih, D.M., et al. 1998. Mice lacking serum paraoxonase are susceptible to organophosphate toxicity and atherosclerosis. *Nature.* **394**:284–287.